The gas phase 1,2-Wittig rearrangement is an anion reaction. A joint experimental and theoretical study

John C. Sheldon, Mark S. Taylor, John H. Bowie,* Suresh Dua, C. S. Brian Chia and Peter C. H. Eichinger

Department of Chemistry, The University of Adelaide, South Australia, 5005, Australia

Received (in Cambridge) 8th July 1998, Accepted 4th December 1998

The migratory aptitudes of alkyl groups in the gas phase 1,2-Wittig rearrangement have been determined experimentally as follows. An anion $Ph–{}^{-}C(OR^1)(OR^2)$, on collisional activation, competitively rearranges to the two 1,2-Wittig ions $PhC(R^1)(OR^2)(O^-)$ and $PhC(R^2)(OR^1)(O^-)$ [R^1 and R^2 = alkyl and $R^1 < R^2$]. These two ions respectively eliminate R^2OH and R^1OH. The smaller alkanol is eliminated preferentially, indicating that R^2 (the larger alkyl group) is migrating preferentially (observed *tert*-Bu > *iso*-Pr > Et > Me): a trend generally taken to indicate a radical reaction. However, a Hammett investigation of the relative losses of MeOH from $R–C_6H_4–{}^{-}C(OMe)_2$ shows this loss decreases markedly as R becomes more electron withdrawing, an observation not consistent with a radical reaction. *Ab initio* calculations [at the CISD/6-311++G**//RHF (and UHF)/6-311++G** levels of theory] have been used to construct potential surface maps for the model 1,2-Wittig systems $^{-}CH_2OMe \rightarrow EtO^-$, and $^{-}CH_2OEt \rightarrow PrO^-$. Each of these exothermic reactions involves migration of an alkyl anion. There are no discrete intermediates in the reaction pathways. There is no indication of a radical pathway for either rearrangement. It is proposed that the gas phase 1,2-Wittig rearrangement involves an anionic migration, and that it is not the barrier to the early saddle point but the Arrhenius *A* factor (or the frequency factor of the QET), which controls the rate of the rearrangement. Weak H-bonding between the alkyl anion and the oxygen of the neutral carbonyl species acts as a pivot in holding the molecular complex together during the migration process. This electrostatic interaction increases with an increase in the number of hydrogens able to H-bond to oxygen and with the number of equivalent ways this H-bonding can occur. The relative migratory aptitude of alkyl anions bound within these molecular complexes is *tert*-Bu^- > *iso*-Pr^- > Et^- ≫ Me^-, an order quite different from the migratory aptitudes of anions expected from thermodynamic considerations. This conclusion indicates that great care must be exercised in utilising thermodynamically derived migratory aptitudes to explain the course of a kinetically controlled reaction in the gas phase.

Introduction

The Wittig rearrangement is one of the better known carbanion rearrangements in solution.[1] It has been proposed that the 1,2-Wittig rearrangement, could, in principle, involve either of the intermediates shown in Scheme 1 (R and R^1 are generally aryl

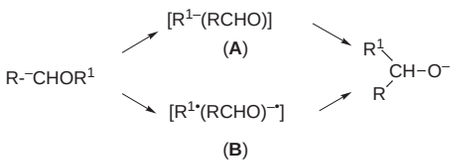

Scheme 1

and alkyl respectively),[1,2] and to support such mechanistic proposals, it has been shown that aldehydes are often byproducts of the reaction.[2] The migratory aptitudes of R′ are in the order of free radical thermodynamic stabilities,[3] thus the radical pair mechanism for the reaction is favoured.[4] However the evidence in favour of a radical reaction is not overwhelming in all cases. For example, when R^1 is chiral, a radical mechanism for the 1,2-Wittig rearrangement (i) demands racemisation of R^1 and this is not always observed,[5] and (ii) should result in the loss of stereochemical integrity in nuclear magnetic resonance CIDNP experiments: *e.g.* as observed for the cognate Stevens rearrangement,[6] but not for the 1,2-Wittig rearrangement.[5] Indeed, it has even been suggested that some 1,2-Wittig rearrangements may have both radical and ionic character.[5]

We have shown that facile 1,2-Wittig rearrangement occurs in the gas phase (*i.e.* in the absence of solvent) for deprotonated benzyl alkyl ethers[7] and a range of cognate anions,[8] but whether these reactions involve radical or anionic rearrangements has not been determined. An *ab initio* study of a model 1,2-Wittig system ($^{-}CH_2OMe \rightarrow EtO^-$) suggests an anionic process through an early transition state with no discrete intermediates in the reaction pathway: the possibility of the analogous radical reaction was not considered in depth.[9] There is also debate concerning the mechanism of the analogous 2,3-Wittig rearrangement. For example, (i) it is not known whether the condensed phase 2,3-Wittig rearrangement of allyl lithiomethyl ether to form homoallyl alcohol is a stepwise or concerted process,[10] while (ii) the gas phase 2,3-(thio)Wittig rearrangement of deprotonated allylthiomethyl ether is suggested to be concerted.[11]

This paper reports the results of a joint experimental/theoretical study planned to determine whether (i) the gas phase 1,2-Wittig rearrangement is stepwise or concerted, and (ii) this rearrangement involves migration of an anion or a radical.

Results and discussion

Experimental studies of $Ph^{-}C(OR^1)(OR^2)$ systems

We have used two experimental methods to attempt to determine whether the gas phase 1,2-Wittig rearrangement involves anionic or radical migration, *viz* (i) the determination of the migratory aptitude of different alkyl groups, and (ii) the way the rearrangement is affected by changing the electrophilicity of

the recipient carbon (of the carbonyl group), *i.e.* a substituent effect study.

(a) The relative migratory aptitudes of alkyl groups. The relative migratory aptitude of two migrating groups can be determined for competitive rearrangements within the same reactant anion. The obvious system for investigation is a deprotonated unsymmetrical benzaldehyde acetal $Ph^-C(OR^1)(OR^2)$ (**C**) where R^1 and R^2 are different migrating groups. The two possible Wittig product ions (**D** and **E**) of this system are shown in Scheme 2. Assuming the migration is rate determining (and

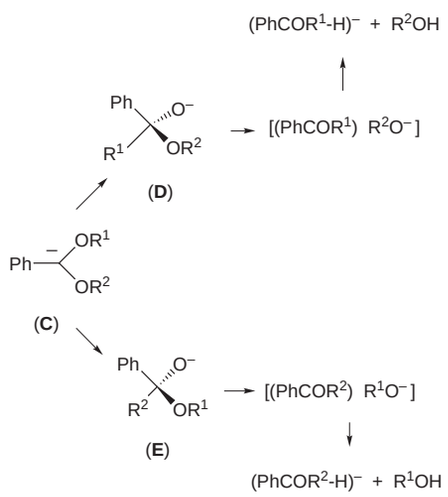

Scheme 2

we will discuss this later), and in the simplest case where R^1 = Me and R^2 = Et, the migratory aptitude of Me^- should be greater than that of Et^-, if previous work in the condensed phase is of relevance here. In the condensed phase, rate and bracketing experiments indicate that the migratory aptitude of alkyl anions is $Me^- > Et^- > iso\text{-}Pr^- > tert\text{-}Bu^-$ in several systems.[12] Alkyl anion migratory aptitudes are not known with certainty for gas phase reactions: thermodynamic migratory aptitudes should, in principle, follow the ΔG°_{acid} values of RH[13] [*i.e.* the smaller the value of ΔG°_{acid} (for the process $RH \rightarrow R^- + H^+$) the higher the migratory aptitude of R^-], *viz* $tert\text{-}Bu^- \sim Me^- > Et^- \sim iso\text{-}Pr^-$. The trend for radicals is different, *i.e.* $Me^\bullet < Et^\bullet < iso\text{-}Pr^\bullet < tert\text{-}Bu$ (the migratory aptitude increases with a decrease in the homolytic bond dissociation energy of RH).[14] For the particular scenario shown in Scheme 2, when R^1 = Me and R^2 = Et, product **E** will be predominant for a radical reaction, whereas **D** will be the major product for an anion reaction.

Since **C**, **D** and **E** are isomeric, we need characteristic fragmentations of **D** and **E** to use as probes in order to determine their relative formation from reactant **C**. Products **D** and **E** should fragment by losses of R^2OH and R^1OH respectively, as shown in Scheme 2: neither of these fragmentations can occur from precursor **C**. In addition, the losses of these alkanols from **D** and **E** will not be involved in the rate determining step (of the sequences shown in Scheme 2) because **D** and **E** are energised [the process **C** to **D** ($R^1 = R^2$ = Me) is calculated to be exothermic by 175 kJ mol^{-1} (using Benson's rules[15] and estimated electron affinities[16]) and if the barrier to the transition state of the 1,2-Wittig rearrangement is of the order of 100 kJ mol^{-1} (*cf.*[9]), the Wittig product ion may have an excess energy of some 275 kJ mol^{-1}. This energy is more than sufficient to both effect formation of the alkoxide anion–neutral complex and subsequent deprotonation within that complex (see Scheme 2)]. Thus the ratios of the losses of R^1OH and R^2OH will not be dependent on the relative basicities of R^1O^- and R^2O^-, but will reflect the relative amounts of **D** and **E** formed from **C**.

Can the above scenario be achieved experimentally? Let us start with the simplest precursor anion, $Ph^-C(OMe)_2$. The reaction between HO^- and $PhCD(OMe)_2$ in the ion source of the VG ZAB 2HF mass spectrometer yields an $(M - D)^-$ ion exclusively. No deprotonation on the phenyl ring is noted. The spectrum of this ion (Fig. 1) shows competitive losses of CH_4 and MeOH. The loss of MeOH is the expected loss from the 1,2-Wittig product ion whereas the loss of CH_4 could, in principle, come directly from the 1,2-Wittig ion (by a process analogous to the loss of ROH shown in Scheme 2), or from a transient intermediate $[(PhCO_2Me)Me^-]$ formed *en route* to the 1,2-Wittig ion. In order to confirm the operation of the 1,2-Wittig rearrangement, we need to compare the decompositions of $Ph^-C(OMe)_2$ with those of independently synthesised $PhC(Me)(OMe)(O^-)$.

We approached the synthesis of $PhC(Me)(OMe)(O^-)$ by using an S_N2 displacement reaction between $PhC(Me)(OMe)_2$ and a range of nucleophiles (including HO^- and MeO^-) in the ion source of the mass spectrometer. Unfortunately, the energised ion $PhC(Me)(OMe)(O^-)$ is not detected in the ion source, thus we could not compare the MS/MS data of this anion with

Table 1 Spectra of product ions from $Ph-^-C(OMe)_2$. Comparison with the spectra of ions formed by independent syntheses

Daughter ion (*m/z*)	Spectrum type	Spectrum CA *m/z* (loss) abundance CR *m/z* (abundance)
(119)	CA	118($H^\bullet$) 100, 77(Ph^-) 10, 41(PhH) 1
	CR	105 (26), 103 (18), 102 (20), 91 (23), 89 (28), 77 (100), 74 (24), 63 (21), 51 (48), 50 (46), 42 (18), 38/39 (9)[a]
$PhCOCH_2^-$ (119)	CA	118($H^\bullet$) 100, 77(Ph^-) 8, 41(PhH) 1
	CR	105 (23), 103 (15), 102 (18), 91 (21), 89 (27), 77 (100), 74 (22), 63 (23), 51 (44), 50 (43), 42 (15), 38/39 (6)[a]
(135)	CA[b]	134($H^\bullet$) 100, 133(H_2) 25, 107(CO) 51, 91(CO_2) 10, 77(Ph^-) 9
	CR	135 (12), 134 (8), 119 (11), 105 (85), 91 (45), 90 (61), 89 (66), 77 (100), 74 (34), 63 (35), 51 (52), 50 (48), 39 (13)
$(C_6H_4)^-$–CO_2Me (135)	CA	134($H^\bullet$) 100, 133(H_2) 18, 107(CO) 45, 105(CH_2O) <5[a], 91(CO_2) 7, 77(Ph^-) 12
	CR	135 (10), 134 (6), 119 (10), 105 (75), 91 (40), 90 (55), 89 (60), 77 (100), 74 (30), 63 (32), 51 (46), 50 (42), 39 (8)

[a] Not resolved. [b] Weak spectrum—peaks of abundance less than 5% are lost in baseline noise.

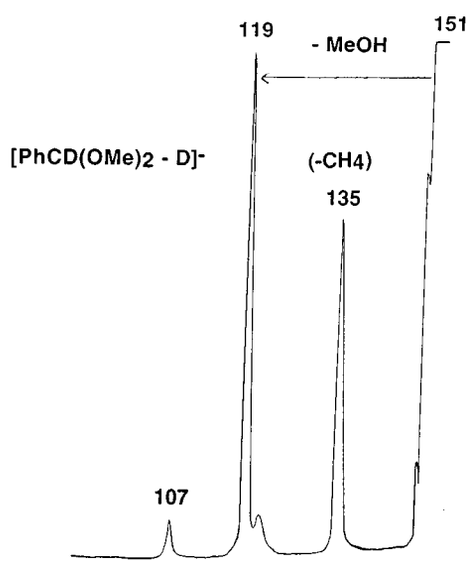

Fig. 1 The collision induced tandem mass spectrum (MS/MS) of $[PhCD(OMe)_2 - D]^-$. VG ZAB 2HF instrument. For experimental procedures see Experimental section.

Table 2 Ratios of R^1OH/R^2OH and R^1H/R^2H losses from Ph–$^-C(OR^1)(OR^2)$ ($R^1 < R^2$)[a]

R^1	R^1	$-R^1OH:-R^2OH$	$-R^1H:-R^2H$
Me	Et	100:8	65:100
Me	*iso*-Pr	100:4	45:100
Et	*iso*-Pr	100:78	88:100
Et	*tert*-Bu	100:60	82:100

[a] Each ratio is an average of five separate determinations. The error is *ca.* ±2%.

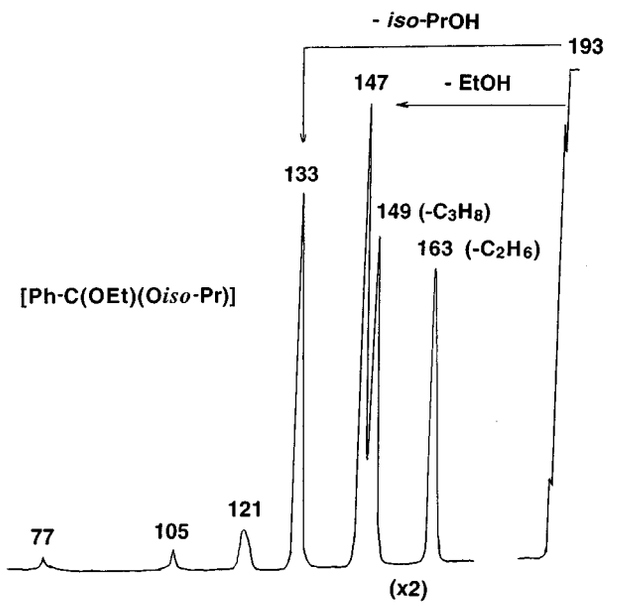

Fig. 2 The collision induced mass spectrum (MS/MS) of Ph–$^-C(OEt)(O$*iso*-Pr). VG ZAB 2HF instrument.

that of $Ph^-C(OMe)_2$. The ion PhC(Me)(OMe)(O^-), on formation in the ion source, decomposes by competitive losses of MeOH and CH_4 to yield pronounced peaks corresponding to $PhCOCH_2^-$ and [(C_6H_4) $^-CO_2Me$] respectively [these source formed ions were identified by their collisional activation (CA) and charge reversal (CR) mass spectra (see Table 1)]. This result is not unexpected since the S_N2 process [$PhC(Me)(OMe)_2$ + $HO^- \rightarrow$ PhC(Me)(OMe)(O^-) + MeOH] is calculated (using Benson's rules[15] and estimated electron affinities[16]) to be significantly exothermic ($\Delta H = -128$ kJ mol^{-1}), as is the subsequent elimination of methanol, *i.e.* PhC(Me)(OMe)$O^- \rightarrow$ $PhCOCH_2^-$ + MeOH ($\Delta H = -280$ kJ mol^{-1}).† We conclude that the loss of MeOH observed in the spectrum of Ph^--$C(OMe)_2$ is a facile process occurring following rearrangement to the energised 1,2-Wittig product anion PhC(Me)(OMe)(O^-).

The spectrum of [$Ph^-C(OEt)(O$*iso*-Pr)] is recorded for illustrative purposes in Fig. 2 while data for a number of deprotonated unsymmetrical benzaldehyde acetals are listed in Table 2. The trend from these spectra is clear: the smaller alkanol is lost preferentially. It is also of interest that the larger alkane is always lost preferentially [although we do not know whether alkane loss is a fragmentation of the Wittig ion, or of an intermediate preceding the formation of the Wittig ion (see earlier)]. The trend for the relative losses of alkanol (for the systems studied) indicates that alkyl migratory aptitudes are *tert*-Bu > *iso*-Pr > Et ⩾ Me. This is the expected ratio of radical migratory aptitudes, consistent with relative rate data for 1,2-Wittig rearrangements in solution.[2–4]

† The ion PhCH(OMe)(O^-), formed by an analogous S_N2 process, is detected in the ion source. In this case the loss of MeOH involves deprotonation of PhCHO, a process less favourable (by some 190 kJ mol^{-1}) than deprotonation of PhCOMe.

Table 3 Ratio of $Me^•$ and MeOH losses in CA MS/MS data from $RC_6H_4-^-C(OMe)_2$

R	σ	$Me^•$	MeOH
p-NMe_2	−0.58	0	100[a]
H	0	[b]	50
p-F	0.15	100	33
m-F	0.34	100	2
p-CN	68	100	0

[a] Source formed ion. No parent ion *p*-$Me_2NC_6H_4COCH_2^-$ is observed in the ion source, thus MS/MS data are not available. [b] Loss of $Me^•$ does not occur when R = H. In this case, loss of CH_4 produces the base peak.

(b) A Hammett substituent effect study. A Hammett type study may assist in differentiating an anionic from a radical mechanism. Consider the summary in Scheme 3, which

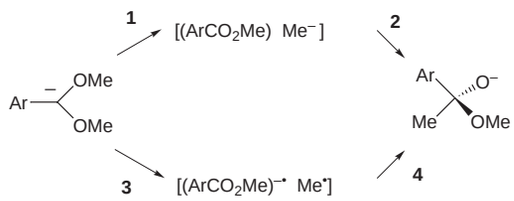

Scheme 3

assumes neither a concerted nor a stepwise process, only that there may be dissociative (**1** or **3**) and/or rearrangement (**2** or **4**) influences on the overall rate of reaction. How will the electronic nature (the Hammett σ value) of a substituent on the phenyl ring affect **1** to **4**? Radical reactions generally show small substituent effects.[17] For this radical reaction, electron withdrawing substituents ($> \sigma$) on the phenyl ring will enhance the rate of dissociation **3** and of migration **4** (electron donating groups will make the radical anion more reactive). The scenario concerning the anionic reaction is different. Firstly, substituent effects for anionic reactions are generally pronounced.[17] In the current case, electron donating substituents ($< \sigma$) will aid dissociation **1**. The situation with regard to migration **2** is not straightforward however. Although electron withdrawing substituents ($> \sigma$) will aid the final approach of the anion to the electrophilic centre, electron donating substituents ($< \sigma$) may facilitate the migration of the anion by the carbonyl moiety 'holding' the migrating anion in place during its circuit to the reactive centre (see later).

The major processes of some substituted species are listed in Table 3. There are problems in using Hammett relationships in gas phase studies.[18] Often there is no inbuilt standard with which the studied process may be related quantitatively. This is true in the current study, and as a consequence, the data must only be used to indicate overall trends. There are only two processes that can be compared, *viz* (i) the loss of $Me^•$, a radical cleavage process of the unrearranged acetal [*i.e.* Ar–$^-C(OMe)_2 \rightarrow [(ArCO_2Me)^{•-}Me^•] \rightarrow (ArCO_2Me)^{•-} + Me^•$], and (ii) the loss of MeOH from the 1,2-Wittig product species. The trends are clear. The loss of $Me^•$ only occurs where there is an electron withdrawing substituent on the ring. The process becomes more pronounced with increasing σ (*i.e.* the loss of $Me^•$ increases as the electron affinity of the neutral ester increases). In contrast, the loss of MeOH decreases dramatically as the electron withdrawing capability of the substituent increases, indeed, there is no loss of MeOH when the substituent is *p*-cyano. These data do not support the proposition that this gas phase 1,2-Wittig rearrangement is a radical process.

We now have the following situation. The generally accepted view is that the condensed phase 1,2-Wittig rearrangement is best explained by a radical mechanism. The published *ab initio* (gas phase) study[9] suggests an anion rearrangement, our experimental (gas phase) migratory aptitudes follow the clas-

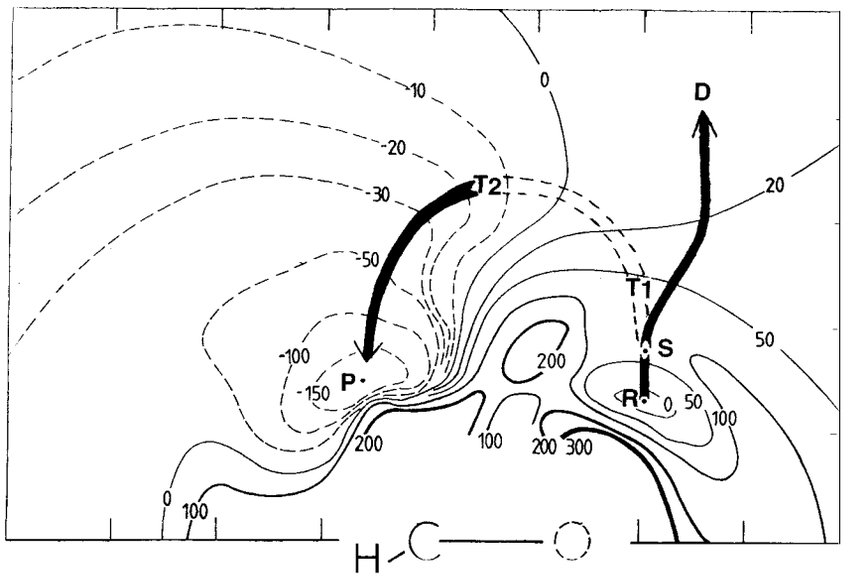

Fig. 3 Potential surface map of the decomposing system $^{-}CH_2OMe$. *Ab initio* calculations at the CISD/6-311++G**//RHF/6-311++G** level of theory.

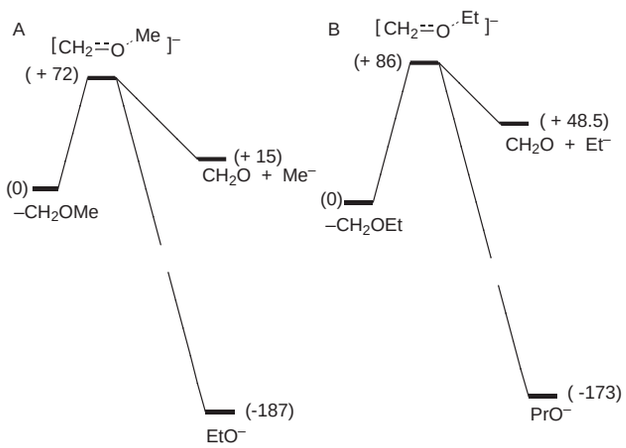

Fig. 4 Reaction coordinate diagram of (**A**) the CH_2O–Me^- and (**B**) CH_2O–Et^- systems. *Ab initio* calculations at the QCISD(T)/6-311++G(d,p)//HF/6-311++G(d,p) level of theory.

sical trends for radicals but not anions, and the (gas phase) Hammett study does not support a radical mechanism. We must now find a mechanism which resolves the (apparently) conflicting experimental evidence, and to do that we must have access to a potential surface map for the gas phase 1,2-Wittig rearrangement.

Potential surfaces for the model systems $^{-}CH_2OR$ to RCH_2O^- (R = Me and Et)

Ab initio calculations of the rearrangement of $^{-}CH_2OMe$ to EtO^- describing the reaction coordinate have already been reported.[9] The data suggest an anionic reaction with an early saddle point but no discrete intermediate. We need to construct a potential surface map for this prototypical system in order to explore the anion mechanism more fully and also to test for the possibility of an alternative radical pathway.‡§ In addition, we wish to compare the methyl migration (of $^{-}CH_2OMe$) with the ethyl migration (of $^{-}CH_2OEt$) in order to ascertain whether the rearrangements proceed by similar or different mechanisms [the electron of Me^- is bound in the free state (E.A. of $Me^{\bullet}$ is 7.5 kJ mol^{-1}),[20] whereas that of Et^- is unbound (E.A. of $Et^{\bullet}$ is −30 kJ mol^{-1})[21]].

The potential surface map for the model 1,2-Wittig rearrangement $^{-}CH_2OMe \rightarrow EtO^-$ is shown in Fig. 3, and is constructed to display the energy and geometry changes which accompany methyl migration from oxygen to carbon. The CISD/6-311++G(d,p)//RHF/6-311++G(d,p) level of theory was used. The corresponding reaction coordinate diagram is shown in Fig. 4: in this case, a higher level of theory, QCISD(T)/6-311++G(d,p)//HF/6-311++G(d,p), was used to represent the major features. Details of geometries and energies of reactant, saddle point and product (shown in Fig. 4) are listed in Table 4. The preferred geometries of reactant and saddle point leading to methyl dissociation possess a plane of symmetry (C_s) through methyl and formaldehyde groups: this plane defines the plane of the map shown in Fig. 3. A point on the map signifies the energy of the rearranging system (in kJ mol^{-1} with respect to CH_3^- and CH_2O at infinite separation)

Table 4 Geometries and energies of reactant, product and transition state for the 1,2-Wittig rearrangements of $^{-}CH_2OMe$ [QCISD(T) 6-311++G(d,p)//HF 6-311++G(d,p) including zero point energy (scaled to 0.9)]. [Me^- = −39.6952202 hartrees; CH_2O = −114.2395661. Me^- + CH_2O = −153.9347863 (nominally 0 kJ mol^{-1} in Fig. 3)]

Reactant	−153.9406641 hartrees	−15.4 kJ mol^{-1}
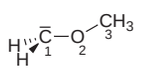	C^1O^2 = 1.476 Å O^2C^3 = 1.371 Å C^3H = 1.123 Å $O^2C^1C^3$ = 114.06°	
Saddle point	−153.9132451 hartrees	+56.6 kJ mol^{-1}
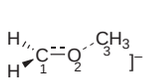	C^1O^2 = 1.257 Å O^2C^3 = 1.961 Å C^3H = 1.087 Å $C^1O^2C^3$ = 113.9°	
Product	−154.0119473 hartrees	−202.6 kJ mol^{-1}
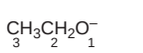	C^1O^2 = 1.325 Å C^1C^3 = 1.550 Å $O^2C^1C^3$ = 114.30°	

‡ It is not feasible to construct a potential surface map of Ph–$^{-}CHOR$ with our facilities. The potential surface map of $^{-}CH_2OMe$ is constructed using 170 different geometries: each geometry (at the level of theory used) needs some 7–8 h of super-computer time. The corresponding time requirement for each calculation of a Ph–$^{-}CHOR$ geometry is >48 h.

§ The radical $^{\bullet}CH_2OMe$ is more stable than the anion:[19] this does not invalidate the use of $^{-}CH_2OMe$ as a model system for the computation of the potential surface for the rearrangement.

Table 5 Geometries and energies of reactant, product and transition state for the 1,2-Wittig rearrangement of $^{-}CH_2OEt$ [QCISD(T) 6-311++G(d,p)//HF 6-311++G(d,p) including zero point energy (scaled to 0.9)]. [Et^{-} = −78.8741163 hartrees; CH_2O = −114.2395661. Et^{-} + CH_2O = −193.1136824]

Reactant	−193.1328663 hartrees	−50.4 kJ mol^{-1}
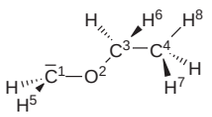	C^1O^2 = 1.478 Å O^2C^3 = 1.371 Å C^3C^4 = 1.526 Å C^1C^5 = 1.102 Å C^3H^6 = 1.094 Å C^4H^7 = 1.088 Å C^4H^8 = 1.092 Å $C^1O^2C^3$ = 113.9° $O^2C^3C^4$ = 109.4°	
Saddle point	−193.0996784 hartrees	+36.8 kJ mol^{-1}
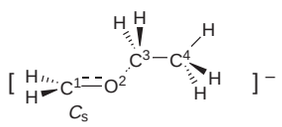	C^1O^2 = 1.249 Å O^2C^3 = 2.021 Å C^3C^4 = 1.499 Å $C^1O^2C^3$ = 116.8° $O^2C^3C^4$ = 150.0°	
Product	−193.198872 hartrees	−223.1 kJ mol^{-1}
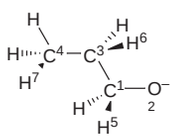	C^1O^2 = 1.325 Å C^1C^3 = 1.550 Å C^3C^4 = 1.531 Å C^1H^5 = 1.124 Å C^3H^6 = 1.091 Å C^4H^8 = 1.091 Å C^4H^7 = 1.090 Å $C^2C^1C^3$ = 143.3°	

when the methyl carbon occupies that point. The notional origin of the 1 Å grid is fixed on the formaldehyde carbon and the lower edge defines the formaldehyde C–O direction.

The potential map of the Me^{-}/CH_2O system is shown in Fig. 3, and is constructed from 170 geometries. The reactant is represented by the shallow local minimum **R** (−26 kJ mol^{-1} relative to Me^{-} and CH_2O at infinite dissociation; O–C(H_3) bond = 1.37 Å). The dissociation to Me^{-} and CH_2O is represented by the arrow **RSD** passing through saddle point **S** [+74 kJ mol^{-1}, O–C(H_3) distance = 1.96 Å]. The most probable continuation of such movement is into the broad flat region leading to Me^{-} plus CH_2O [Me^{-} will eventually eject an electron to give $Me^{\bullet}$ since the excess energy of the system is greater than the E.A. of $Me^{\bullet}$ (7.5 kJ mol^{-1})]. The rearrangement channel from **S** through $\mathbf{T_1}$ to $\mathbf{T_2}$ ($\mathbf{T_1}$ and $\mathbf{T_2}$ are transit structures, the relevance of which will be described later) is not well defined: thereafter, the descending channel to the product **P** is well defined. There is no discrete intermediate along the reaction coordinate. The map demonstrates that the 1,2-Wittig rearrangement of $^{-}CH_2OMe$ is inefficient (with respect to dissociation to Me^{-} and CH_2O) since few methyl groups departing from saddle point **S** will enter channel $\mathbf{T_1T_2P}$ unless the forces of association within the anion complex are favourable in directing the course of that reaction (see later).

Migration of a methyl radical also needs to be considered, as well as the possibility of a rearrangement that might have both anion and radical character and different stages of the migration (*cf.*[5]). These possibilities were explored by re-examining structures in the vicinity of the reaction coordinate using unrestricted Hartree–Fock calculations (the electronic state here is still a singlet, but electrons can be assigned to separate molecular orbitals to model a homolytic bond breaking and the emergence of diradical character). The results from the RHF and UHF calculations are identical: there is no indication of any radical/radical anion pathway either preceding or following saddle point **S**.

We have not computed a full potential surface map (like that shown in Fig. 3) for the homologous system $^{-}CH_2OEt \rightarrow PrO^{-}$.¶ However we have studied the analogous region to that bounded by **R**, **S**, $\mathbf{T_1}$, $\mathbf{T_2}$ and **P** in Fig. 3. In this region, the surface is visually very similar to that shown in Fig. 3. This reaction involves migration of an ethyl anion bound within the molecular complex. UHF calculations again fail to uncover any indication of a radical/radical anion pathway. The geometries and energies of reactant, saddle point and product have also been calculated at the higher level of theory [QCISD(T)/6-311++(d,p)//6-311++G(d,p)]. These data are summarised in Fig. 4, with details of relevant geometries and energies listed in Table 5. The difference in saddle point energies are 10, 10.5 and 14 kJ mol^{-1} respectively for the following levels of theory: HF/6-311++G(d,p), CISD/6-311++G(d,p) and QCISD(T)/6-311++ G(d,p). Thus the barrier to the transition state for the Et^{-} migration is calculated to be 14 kJ mol^{-1} higher than that for the corresponding Me^{-} migration at the highest level of theory used.

An anionic migration

Ab initio calculations indicate that the gas phase 1,2-Wittig reactions of two model systems are anionic rearrangements. The experimental results of the Hammett study are not consistent with a radical mechanism. How then can we explain the experimental alkyl migratory aptitudes which are apparently consistent with a radical process, but not with the classical relative migratory aptitudes expected of anions. The clue to this problem is to be found in the potential surface shown in Fig. 3, and with the analogous, but partial surface, that has been constructed for the cognate system $^{-}CH_2OEt \rightarrow PrO^{-}$. These surfaces exhibit subtle differences which cannot be seen when the maps are represented as shown in Fig. 3. The first difference between the two processes is that the barrier for the 1,2-Wittig rearrangement of $^{-}CH_2OEt$ is 14 kJ mol^{-1} higher than that for the analogous reaction of $^{-}CH_2OMe$. If these barriers determine migratory trends, Me^{-} must migrate faster than Et^{-}. This is the reverse of what is observed experimentally. Thus it cannot be the modest barriers to the early transition states which are causing the pronounced difference noted in the migratory aptitudes of Me and Et.

The rate of a gas-phase reaction is dependent on both the barrier to the saddle point and the Arrhenius *A* factor[22] (or the frequency factor of the QET expression) (see[23] for an illustration of the importance of this parameter). If the reaction proceeds through the saddle point **S** in an upward direction in Fig. 3, there is an arc of some 60° where decomposition may be effected to yield Me^{-} and CH_2O. In contrast, the competitive formation of EtO^{-} has a low probability relative to dissociation to Me^{-} and CH_2O. In this system, it is not the barrier from **R** to **S** which is the major factor influencing the rate of reaction, it is the low frequency factor of the migration stage of this process, even though migration is occurring as part of a synchronous reaction at a stage of rapid energy descent. Any feature which affects the frequency factor will alter the rate of this reaction.

When particular details of the two potential surfaces are compared it is clear why the migration of Et^{-} is more efficient than that of Me^{-}. We have arbitrarily chosen two transit points on the rearrangement reaction coordinate of each potential surface map to illustrate particular features of the molecular rearrangements. We have called these transit points $\mathbf{T_1}$ and $\mathbf{T_2}$ (see Fig. 3). The $\mathbf{T_1}$ structures immediately follow the saddle points on the rearrangement reaction coordinate on each potential surface map and are in identical positions, *i.e.* they have the same significant coordinates. The geometries of these $\mathbf{T_1}$ structures are shown for comparison, in Fig. 5. There is a weak electrostatic interaction between the electron rich oxygen

¶ Calculation of each geometry for this system required some 24–26 h of super-computer time.

Table 6 Mulliken charge analysis of HF/6-311++G(d,p) wavefunctions of transit structures $\mathbf{T_2}$ shown in Figs. 6 and 7

$\mathbf{T_2}$	H-bonding	Carbanion C	β Carbon	$C(CH_2O)$	$C(CH_2O)$
Methyl	+0.068	−1.008		+0.246	−0.337
Ethyl	+0.091	−0.752	−0.418	+0.226	−0.280
iso-Propyl	+0.068[a]	−0.117	−0.587[b]	+0.156	−0.284
	+0.079[c]		−0.442[d]		
tert-Bu	+0.133	0.555	−0.563[e]	+0.143	−0.278
			−0.744[f]		

[a] For bonding H that has shorter distance to O (see Fig. 7). [b] For bonding H that has longer distance to O. [c] For the carbon of the methyl group that is involved in H-bonding. [d] For the carbon of the methyl group that is not involved in H-bonding. [e] For the two equivalent methyl groups not involved in H-bonding. [f] For the methyl group involved in H-bonding.

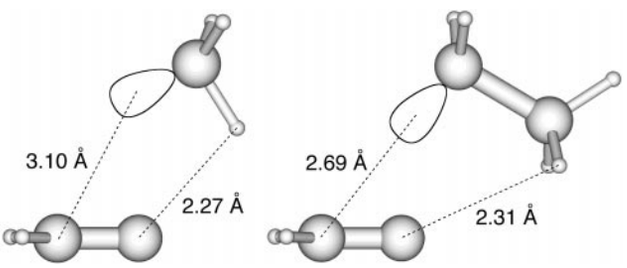

Fig. 5 Comparison of transit structures $\mathbf{T_1}$ for the migrating systems (**A**) [Me^-/CH_2O] and (**B**) [Et^-/CH_2O]. *Ab initio* calculations at the QCISD(T)/6-311++G(d,p)//HF/6-311++G(d,p) level of theory.

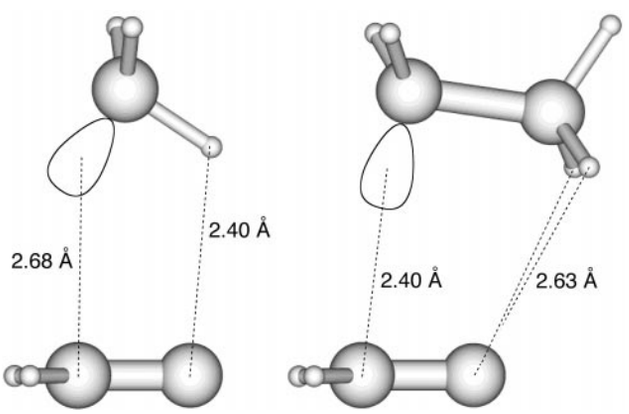

Fig. 6 Comparison of transit structures $\mathbf{T_2}$ for the migrating systems (**A**) [Me^-/CH_2O] and (**B**) [Et^-/CH_2O]. *Ab initio* calculations at the QCISD(T)/6-311++G(d,p)//HF/6-311++G(d,p) level of theory.

(of formaldehyde) and one hydrogen of the methyl anion. For the ethyl anion complex, the hydrogen bonding is to two of the methyl hydrogens of the substituent α to the carbanion centre: an electrostatic interaction which is greater than that for the corresponding methyl anion migration.

Transit structure $\mathbf{T_2}$ (for the Me^-/CH_2O system) is chosen to illustrate the geometry of the rearranging system *en route* to products (see $\mathbf{T_2}$ on the potential surface map shown in Fig. 3). This structure is shown in Fig. 6. The point with the same significant coordinates on the Et^-/CH_2O surface is also shown in Fig. 6. Hydrogen bonding between the anion and neutral essentially acts as a pivot during the anion migration towards the electrophilic carbon terminus. The acidic nature of the hydrogens involved in the H-bonding are substantiated by the Mulliken electron density analyses of transit structures $\mathbf{T_2}$ listed in Table 6. Thus Et^- migrates more efficiently than Me^- in these systems, a result opposite to that expected using thermodynamic anionic migratory aptitudes. This enables the rationalisation of the relative migratory aptitudes of Et^- and Me^- in this reaction, but what accounts for the further trend *tert*-Bu^- > *iso*-Pr^- > Et^-? The answer to this is also provided by a knowledge of the appropriate transit structures. In order to answer this question, we have computed the transit structures $\mathbf{T_2}$ for the *iso*-Pr^-/CH_2O and *tert*-Bu^-/CH_2O systems: these are

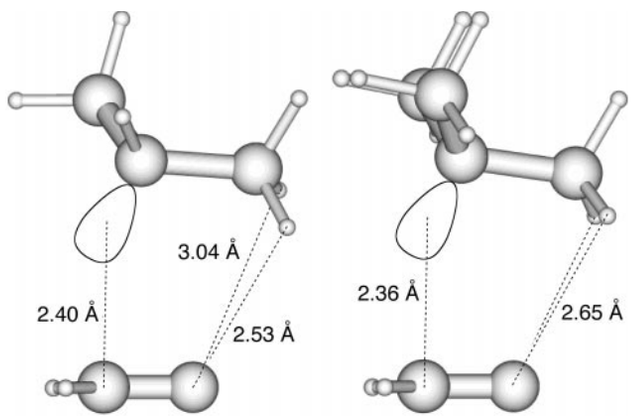

Fig. 7 Transit structures $\mathbf{T_2}$ for the migrating systems [*iso*-Pr^-/CH_2O] (left) and [*tert*-Bu^-/CH_2O]. *Ab initio* calculations at the QCISD(T)/6-311++G(d,p)//HF/6-311++G(d,p) level of theory.

modelled using the same significant coordinates as those of the Et^-/CH_2O transit structure $\mathbf{T_2}$ and are shown in Fig. 7. The lowest energy structure in both cases is one where H-bonding is initiated from only one methyl group, but in the *iso*-Pr case the two hydrogen bonds are not equivalent (see Fig. 7).‖ We propose that migrating *iso*-propyl and *tert*-butyl anions are held in place by an H-bonding pivot occurring between two hydrogens of one methyl group and the oxygen of formaldehyde. The migratory aptitudes in these cases are also influenced by the reaction path degeneracy, *i.e.* the number of degenerate structures that can be drawn for each transit structure (*i.e.* in the ratio 3:2:1 for *tert*-Bu, *iso*-Pr and Et respectively) (for a discussion of reaction path degeneracy see[24]). The migratory aptitudes are thus *tert*-Bu^- > *iso*-Pr^- > Et^-.

Conclusions

We propose that the gas phase 1,2-Wittig rearrangement is an anionic reaction. The saddle point is reactant like (*i.e.* only minor dissociation of the O–C bond has occurred in attaining the saddle point), and there is no discrete intermediate formed during the reaction. The migration which proceeds following formation of the saddle point has a low frequency factor: this is the major influence on the rate of reaction. During the migration process, the migrating anion is held, by weak hydrogen bonding, to the neutral to which the anion is migrating. The efficiencies of these reactions are a function of the extent of the H-bonding that holds the anion and neutral together during the initial phase of the migration, together with the reaction degeneracy of the migration pathway. Once the molecular complex has reached $\mathbf{T_2}$ (see Fig. 3), the subsequent nucleophilic substitution should be efficient for all the systems

‖ The structure shown for the *iso*-Pr^-/CH_2O system in Fig. 7 is 32 kJ mol^{-1} more negative in energy [at the QCISD(T)6-311++G(d,p)//HF/6-311++G(d,p) level of theory] than the analogous transit structure in which both methyl groups are involved equally in the H-bonding.

studied. The relative kinetic migratory aptitudes of alkyl groups in this rearrangement are *tert*-$Bu^- > iso$-$Pr^- > Et^- \gg Me^-$.

Experimental

Mass spectrometric methods

Collisional activation (CID) mass spectra (MS/MS) were determined with a VG ZAB 2HF mass spectrometer.[25] Full operating details have been reported.[26] Specific details were as follows: the chemical ionisation slit was used in the chemical ionisation source, the ionising energy was 70 eV, the ion source temperature was 100 °C, and the accelerating voltage was 7 kV. The liquid samples were introduced through the septum inlet with no heating [measured pressure of sample 1×10^{-6} Torr (1 Torr = 133.322 Pa)]. Deprotonation was effected using HO^- (from H_2O: measured pressure 1×10^{-5} Torr). The estimated source pressure was 10^{-1} Torr. CID MS/MS data were obtained by selecting the particular anion under study with the magnetic sector, passing it through the collision cell, and using the electric sector to separate and monitor the product ions. Argon was used as collision gas in the second collision cell (measured pressure, outside the cell, 2×10^{-7} Torr), giving a 10% reduction in the main beam, equivalent to single collision conditions. Charge reversal (CR) mass spectra were measured as for CID MS/MS (above) except that the voltages of the electric sector were reversed to allow transmission of positive ions.[27]

Syntheses of labelled and unlabelled compounds

The dimethyl and diethyl acetals of benzaldehyde were commercial samples. The following acetals were prepared by reported procedures: $RC_6H_4(OMe)_2$: *m*-F,[28] *p*-F,[29] *p*-CN[29] and *p*-NMe_2.[30] The dimethyl ketal of acetophenone was prepared by a reported method.[30]

3-Cyanobenzaldehyde dimethyl acetal was prepared by a standard method[29] as a colourless liquid (bp 154–155 °C/17 mm Hg, 64% yield). Found: C, 67.87; H, 6.07; N, 7.96%; $C_{10}H_{11}NO_2$ requires C, 67.78; H, 6.25; N, 7.90%. ^{1}H NMR [δ ppm, 300 MHz (in $CDCl_3$)] 3.33 (s, 6H, OCH_3), 5.43 (s, 1H, C–H), 7.4–7.8 (m, 4H, aromatic H). *m*/*z* 182 ($M^{\bullet+}$, 6%), 151 ($-MeO^{\bullet}$, 100%), 135 ($MeOC_6H_4CO^+$, 32%).

Benzaldehyde-α-$^2H_1$ dimethyl acetal was prepared from benzaldehyde-α-$^2H_1$ by a reported method[31] in 77% yield ($^2H_1$ = 99%).

The mixed acetals (see Table 3). General procedure. Benzaldehyde dimethyl (or diethyl) acetal (2.5 g) was added to the appropriate alcohol (0.75 g) containing sulfuric acid (concentrated, 2 drops). The mixture was allowed to stir at 100 °C under nitrogen for 30 min, quenched with sodium metal, and extracted with diethyl ether (2×15 cm^3). Removal of the solvent *in vacuo* followed by vacuum distillation of the residue yielded a mixture of $PhCH(OR^1)_2$, $PhCH(OR^1)(OR^2)$ and $PhCH(OR^2)_2$ which was not separated. Injection of a sample of this mixture into the mass spectrometer, followed by reaction with HO^- in the ion source of the VG ZAB 2HF yielded the three $(M - H)^-$ ions. The required ion $Ph-{}^-C(OR^1)(OR^2)$ was selected using the magnetic sector: collisional activation MS/MS data were obtained as described above.

Ab initio calculations

Ab initio calculations of all stable species (local minima) and the transition state shown in the potential surface map (Fig. 3) were determined with GAUSSIAN92[32] with restricted Hartree–Fock wave functions [RHF/6-311++G**]. The geometries of stable species were optimised with initial force constants analytically computed. The final geometries were found to have no imaginary frequencies. The optimisations of transition states were computed with analytical force constants throughout. A transition state is characterised by possessing only one imaginary frequency and its Hessian matrix possesses only one negative eigen value. The remaining points (other than the stationary points) used to construct the potential surface are selected and fixed positions of the carbanion carbon relative to the C–O bond. These selected points on the surface effectively freeze just two of the molecular coordinates, that is, the vertical and horizontal displacement of the carbanion carbon from the carbonyl carbon. Final energies were determined at the CISD/6-311++G**//RHF/6-311++G** level of theory. A number of key structures on the surface were also computed at the unrestricted Hartree–Fock (UHF) level of theory.

Ab initio calculations of stable species and transition states shown in Fig. 4 were determined with GAUSSIAN94[33] using the QCISD(T)/6-311++G(d,p)//HF/6-311++G(d,p) level of theory. Vibrational zero point energy corrections have been made.

Acknowledgements

We thank the Australian Research Council for financial support. One of us (S. D.) thanks the ARC for a research associate position.

References

1 W. Schlenk and E. Bergmann, *Justin Liebigs Ann. Chem.*, 1928, **464**, 22; G. Wittig and L. Lohmann, *Justin Liebigs Ann. Chem.*, 1942, **550**, 260; G. Wittig, *Angew. Chem.*, 1954, **66**, 10; H. E. Zimmerman, in *Molecular Rearrangements*, ed. P. DeMayo, Interscience, Vol. 1, p. 345, 1963; J. E. Baldwin, J. DeBernardis and J. E. Patrick, *Tetrahedron Lett.*, 1970, 353.
2 C. R. Hauser and S. W. Kantor, *J. Am. Chem. Soc.*, 1951, **73**, 1437; J. Cast, T. S. Stevens and J. Holmes, *J. Chem. Soc.*, 1960, 3521.
3 P. T. Lansbury, V. A. Pattison, J. D. Sidler and J. B. Bierber, *J. Am. Chem. Soc.*, 1966, **88**, 78; H. Schafer, U. Schöllkopf and D. Walter, *Tetrahedron Lett.*, 1968, 2809; T. Weiske and H. Schwarz, *Tetrahedron*, 1986, **42**, 6245, and references cited therein.
4 U. Schöllkopf, *Angew. Chem., Int. Ed. Engl.*, 1970, **9**, 763.
5 J. F. Garst and C. D. Smith, *J. Am. Chem. Soc.*, 1976, **98**, 1526.
6 R. A. W. Johnstone and T. S. Stevens, *J. Chem. Soc.*, 1960, 3340; J. J. Eisch, S. K. Dua and C. A. Kovacs, *J. Org. Chem.*, 1987, **52**, 4437, and references cited therein.
7 P. C. H. Eichinger, J. H. Bowie and T. Blumenthal, *J. Org. Chem.*, 1986, **51**, 5078.
8 P. C. H. Eichinger and J. H. Bowie, *J. Chem. Soc., Perkin Trans. 2*, 1987, 1499; P. C. H. Eichinger and J. H. Bowie, *J. Chem. Soc., Perkin Trans. 2*, 1988, 497; P. C. H. Eichinger and J. H. Bowie, *J. Chem. Soc., Perkin Trans. 2*, 1990, 1763.
9 P. Antoniotti and G. Tonachini, *J. Org. Chem.*, 1993, **58**, 3622.
10 Y.-D. Wu, K. N. Houk and J. A. Marshall, *J. Org. Chem.*, 1990, **55**, 1421.
11 M. R. Ahmad, G. D. Dahlke and S. R. Kass, *J. Am. Chem. Soc.*, 1996, **118**, 1398.
12 G. B. Ellison and P. C. Engelking, *J. Chem. Phys.*, 1978, **69**, 1826.
13 C. H. DePuy, V. M. Bierbaum and R. Damrauer, *J. Am. Chem. Soc.*, 1984, **106**, 4051.
14 J. Fossey, D. Lefort and J. Sorba, *Free Radicals in Organic Chemistry*, Wiley, New York, 1995, pp. 31–38.
15 S. W. Benson, *Thermochemical Kinetics*, Wiley, New York, London and Sydney, 1968.
16 NIST Standard Reference Database - March 1998. Electron Affinities.
17 F. Ruff and I. G. Csizmadia, *Organic Reactions, Equilibria, Kinetics and Mechanism*, Elsevier, Amsterdam, 1994, pp. 161–210.
18 K. Levsen, *Fundamental Aspects of Organic Mass Spectrometry*, Verlag Chemie, Weinheim and New York, 1978, p. 119.
19 C. H. DePuy, V. M. Bierbaum and R. Damrauer, *J. Am. Chem. Soc.*, 1984, **106**, 4051.
20 D. E. Applequist and D. F. O'Brien, *J. Am. Chem. Soc.*, 1963, **85**, 743; R. E. Dessy, W. Kitching, T. Psarras, R. Salinger, A. Chen and T. Chivers, *J. Am. Chem. Soc.*, 1966, **88**, 460; A. I. Shatenshtein, *Adv. Phys. Org. Chem.*, 1963, **1**, 156.
21 G. B. Ellison, P. C. Engelking and W. C. Lineberger, *J. Am. Chem. Soc.*, 1978, **100**, 2556; C. H. DePuy, V. M. Bierbaum and R. Damrauer, *J. Am. Chem. Soc.*, 1984, **106**, 4051; see also S. G. Lias, J. E. Bartmess, J. F. Liebman, J. L. Holmes, R. D. Levin and W. G. Mallard, Gas Phase Ion and Neutral Thermochemistry, *J. Phys. Chem. Ref. Data 17*, 1988, Suppl. 1 (the computer version was used).

22 G. W. Castellan, *Physical Chemistry*, Addison-Wesley Publ. Co., Amsterdam, 1983, 3rd edn., pp. 813, 858.
23 S. Okada, Y. Abe, S. Tanaguchi and S. Yamabe, *J. Am. Chem. Soc.*, 1987, **109**, 295.
24 For discussions of reaction path degeneracy see: P. J. Robinson and K. A. Holbrook, *Unimolecular Reactions*, Wiley Interscience, New York, 1972, pp. 80–85; R. G. Gilbert and S. C. Smith, *Theory of Unimolecular and Recombination Reactions*, Blackwell Scientific Publications, Oxford, UK, 1990, pp. 87–98.
25 V. G. Instruments, Wythenshawe, Manchester, UK, Model ZAB 2HF.
26 M. B. Stringer, J. H. Bowie and J. L. Holmes, *J. Am. Chem. Soc.*, 1986, **108**, 3888.
27 J. H. Bowie and T. Blumenthal, *J. Am. Chem. Soc.*, 1975, **97**, 2959; J. E. Szulejko, J. H. Bowie, I. Howe and J. H. Beynon, *Int. J. Mass Spectrom. Ion Phys.*, 1980, **13**, 76.
28 J. N. Frescos, G. W. Morrow and J. S. Swenton, *J. Org. Chem.*, 1985, **6**, 805.
29 T. Sigeru, I. Tsutoma, T. Sadahito, H. Hirofimi, K. Hideki and U. Kenji, *Bull. Chem. Soc. Jpn.*, 1987, **60**, 2173.
30 I. Fleming, J. Iqbal and E. P. Krebs, *Tetrahedron*, 1983, **39**, 841.
31 J. Klein and E. D. Bergmann, *J. Am. Chem. Soc.*, 1957, **79**, 3452.
32 M. J. Frisch, G. W. Trucks, M. Head-Gordon, P. M. W. Gill, M. W. Wong, J. B. Foresman, B. J. Johnson, H. B. Schlegel, M. A. Robb, E. S. Replogle, R. Gomperts, J. L. Andres, K. Raghavachari, J. S. Binkley, C. Gonzalez, R. L. Martin, D. J. Fox, D. J. Defrees, J. Baker, J. J. P. Stewart and J. A. Pople, GAUSSIAN92, Revision G3, Gaussian Inc., Pittsburgh, PA, 1992.
33 M. J. Frisch, G. W. Trucks, H. B. Schlegel, P. M. W. Gill, B. G. Johnson, M. A. Robb, J. R. Cheeseman, T. Keith, G. A. Petersson, J. A. Montgomery, K. Raghavachari, M. A. Al-Latham, V. G. Zakrewski, J. V. Ortiz, J. B. Foresman, J. Cioslowski, B. B. Stefanov, A. Nanayakkara, M. Challacombe, C. Y. Peng, P. V. Ayala, W. Chem, M. W. Wong, J. L. Andres, E. S. Replogle, R. Gomperts, R. L. Martin, D. J. Fow, J. S. Binkley, D. J. Defrees, J. Baker, J. P. Stewart, M. Head-Gordon, C. Gonzales and J. A. Pople, GAUSSIAN94, Revision C3, Gaussian Inc., Pittsburgh, PA, 1995.

Paper 8/05319G